Oscillatory modes of extended Nile River records (A.D. 622–1922)

D. Kondrashov,[1] Y. Feliks,[1,2] and M. Ghil[1,3]

The historical records of the low- and high-water levels of the Nile River are among the longest climatic records that have near-annual resolution. There are few gaps in the first part of the records (A.D. 622–1470) and larger gaps later (A.D. 1471–1922). We apply advanced spectral methods, Singular-Spectrum Analysis (SSA) and the Multi-Taper Method (MTM), to fill the gaps and to locate inter-annual and interdecadal periodicities. The gap filling uses a novel, iterative version of SSA. Our analysis reveals several statistically significant features of the records: a non-linear, data-adaptive trend that includes a 256-yr cycle, a quasi-quadriennial (4.2-yr) and a quasi-biennial (2.2-yr) mode, as well as additional periodicities of 64, 19, 12 and, most strikingly, 7 years. The quasi-quadriennial and quasi-biennial modes support the long-established connection between the Nile River discharge and the El-Niño/Southern Oscillation (ENSO) phenomenon in the Indo-Pacific Ocean. The longest periods might be of astronomical origin. The 7-yr periodicity, possibly related to the biblical cycle of lean and fat years, seems to be due to North-Atlantic influences.

1. Introduction

Pharaonic and medieval Egypt depended solely on winter agriculture and hence on the summer floods. The rise of the waters of the Nile was measured therefore regularly from the earliest times [*Said*, 1993]. Several authors compiled the annual maxima and minima of the water level recorded at nilometers in the Cairo area, in particular at Rodah Island, from A.D. 622 to 1922. The most complete records for the time since the Arab invasion (A.D. 622 = A.H. 1) [*Toussoun*, 1925; *Ghaleb*, 1951; *Hurst*, 1952] were corrected to account for changes in the unit of length used (the cubit), the rise of the bed of the Nile through siltation, and the differences in lunar and solar calendars by *Popper* [1951].

Climate researchers have studied extensively the resulting multi-century, annually resolved records and have demonstrated the significant association between the rainfall in the catchment area of the Nile tributaries, the Indian monsoon, and ENSO [*Walker*, 1910; *Quinn*, 1992]. A recent weakening of the close relationship between ENSO and the Indian monsoon [*Kumar et al.*, 1999], however, might foreshadow a

similar weakening of the East-Africa–ENSO correlation. In any case, some regularities in the Nile River records cannot be explained by the ENSO connection. In particular, North Atlantic influences over North Africa and the Middle East have been detected in several geologic [*Felis et al.*, 2004] and historical [*Mann*, 2002] time series, and may extend all the way into the Nile River's source area, further to the south. To ascertain whether this is so, we apply advanced methods for the filling of gaps in the records and for their spectral analysis with appropriate confidence tests.

Said [1993] reviewed many studies that applied Fourier analysis [*Hameed*, 1984] to the discharge records and noted they all agree on the presence of periodicities, but differ in the exact values of the periods. Recent studies, using more advanced spectral methods, reexamined these records. Thus *De Putter et al.* [1998] applied the classical version of MTM [*Thomson*, 1982], with a white-noise significance test, to both the low- and high-water records at Rodah Island for A.D. 622–1470. They found significant periodicities in both records at 76, 21, and 13 yr, in the low-water record at 256 yr and in the high-water record at 5 yr. These authors also applied evolutionary MTM to the records and showed the shift or disappearance of certain spectral peaks at different epochs, in particular of certain low-frequency peaks during the Medieval Warm Period in Europe (∼A.D. 950–1250).

Our work provides five important new results on the interannual, interdecadal and centennial evolution of climate in northeast Africa over the last millennium-and-a-half: (i) a complete 1300-yr record of Nile River floods with annual resolution that permits one to study the evolution of the regularities over the most recent 450 years (A.D. 1471–1922); (ii) more robust statistical-significance tests; (iii) an analysis of the net flood record; (iv) sharper and more reliable determination of climatic-regime transitions; and (v) evidence for a novel source of interannual climatic variability for tropical East Africa, namely changes in the North Atlantic ocean circulation.

2. Data and Methods

2.1. Data

We used several versions of the high- and low-water records: those given in the Table occupying pp. 366–404 of *Toussoun* [1925], as well as the records corrected by *Popper* [1951], who used the compilation of *Ghaleb* [1951], along with Toussoun's data. After filling the gaps in the latter part of the records (A.D 1471–1922) (see below), we carried out analyses on both the short (A.D. 622–1470) and the long (A.D. 622–1922) records. In addition, we examined the difference between the high- and low-water records, which we argue is a better proxy record for the Nile floods than the high-level time series.

2.2. Spectral Methods

We apply advanced, well-documented spectral method to estimate the regularities in our data sets. SSA arises from an interest in connecting nonlinear dynamics with time series analysis [*Broomhead and King*, 1986], while MTM is

---

[1]Department of Atmospheric and Oceanic Sciences and Institute of Geophysics and Planetary Physics, University of California, Los Angeles, U.S.A.

[2]Mathematics Department, Israel Institute for Biological Research, Ness-Ziona, Israel.

[3]Département Terre-Atmosphère-Océan and Laboratoire de Météorologie Dynamique/IPSL, Ecole Normale Supérieure, F-75231 Paris Cedex 05, FRANCE.

based on the optimization of spectral-leakage-resistant filters [*Thomson*, 1982].

SSA is a data-adaptive, non-parametric spectral method based on diagonalizing the lag-covariance matrix of a time series [*Colebrook*, 1978; *Fraedrich*, 1986; *Vautard and Ghil*, 1989]. The eigenvectors of this matrix are the empirical orthogonal functions (EOFs) and projection onto them yields the corresponding principal components. The entire time series or parts of it that correspond to trends, oscillatory modes or noise can be reconstructed by using linear combinations of these principal components and EOFs, which provide the reconstructed components (RCs) [*Ghil and Vautard*, 1991; *Ghil et al.*, 2002].

Our significance tests are carried out with respect to red noise, since the Nile River records, like most climatic and other geophysical time series, have larger power at lower frequencies. The main methods we used are the Monte Carlo version [*Allen and Smith*, 1996] of SSA [*Vautard et al.*, 1992] and the robust MTM version for both line and background estimation [*Mann and Lees*, 1996], as provided in version 4.2 of the SSAMTM Toolkit [*Ghil et al.*, 2002] (see also the freeware toolkit documentation at http://www.atmos.ucla.edu/tcd/ssa/).

2.3. Gap filling by iterative SSA

Analyzing the full extent of the available water-level records, with the missing points filled in, allows for greater accuracy and better significance testing in the spectral analysis. It also improves our knowledge on the evolution of the oscillatory modes over the entire 13 centuries of record and especially over the last 450 years.

Schoellhamer [2001] first suggested using SSA to obtain spectral estimates from records with a large fraction of missing data. The method applied here differs from his in two ways: (i) we iteratively produce estimates of missing data points, which are then used to compute a self-consistent lag-covariance matrix and its empirical orthogonal functions (EOFs); and (ii) we use cross-validation to optimize the window width and number of dominant SSA modes to fill the gaps. The full procedure and the tests on both synthetic and geophysical data will appear in a more detailed paper, currently in preparation.

3. Results and Discussion

First, we consider the traditionally used, short Nile River records (A.D. 622–1470), where a few missing data points have been linearly interpolated (see Fig. 1a). Next, we apply our iterative gap-filling algorithm to estimate the missing data in the extended Nile River records (A.D. 622–1922). The low- and high-water records are strongly correlated in the low-frequency range (periods of 50 yr and longer), so we apply multi-channel SSA [*Ghil et al.*, 2002] to fill the gaps in either record. Using the 9 leading EOFs of the two-channel SSA minimizes the estimation error of 50 independent cross-validation experiments; these 9 EOFs capture a slight upward trend, accompanied by a very low-frequency oscillation with a 256-yr period, and a 64-yr mode. A 100-yr window minimizes the cross-validation error overall. The extended low- and high-water records, with the missing points filled in, appear in Fig. 1b. The nonlinear, data-adaptive upward trend in both the short and extended records might be due to siltation [*Popper*, 1951].

To better study interannual and interdecadal periodicities, we first remove the lowest-frequency component (*i.e.*, the trend + 256-yr oscillation). This combination is captured in both short and extended records by the two leading eigenmodes of the SSA analysis with a 100-yr window. Next, we apply Monte Carlo SSA with a window of $M = 75$

yr to the detrended time series. Very similar results have been obtained within a range of 65 yr $\leq M \leq$ 90 yr (not shown). We also apply MTM with $K = 7$ tapers, which yields a spectral resolution of 0.009 cycle/yr, and use a cutoff at the 95% significance level for both methods.

Tables 1a,b display the spectral results for the short and extended record, respectively. The periods are nearly identical in both types of records. This similarity is not surprising for the longest period in the two tables, since the 64-yr mode was used in the gap filling. But the very close results for the shorter periods, namely 18–19 yr, 7.2–7.3 yr and the ENSO-window peaks is remarkable, since the extended records do contain independent information on these periods.

The 7-yr mode in the high-water and difference records, both short and extended, is quite robust and does not seem to have been previously discussed, aside from a parenthetical reference to an 8.1-yr peak in the high-water record of *De Putter et al.* [1998].

A 7–8-yr peak exists in instrumental records of North Atlantic sea surface temperatures [*Moron et al.*, 1998] and sea level pressure [*Da Costa and Colin de Verdière*, 2002], as well as in the North Atlantic Oscillation index [*Wunsch*, 1999]. *Felis et al.* [2004] have shown 5–6-yr variability to persist in isotopic coral records from the northernmost Red Sea (Gulf of Aqaba) during the last interglacial, 120 kyr ago. *Mann* [2002] has found 8–9-yr variability in an index of Middle-and-Near East temperature, back to 1750 or 1650 A. D. Our clear and persistent 7-yr peak for the extended Nile River records (A.D. 622–1922) demonstrates the extent of North-Atlantic influences over the last millennium-and-a-half, all the way into Eastern Africa's tropical regions.

The spatio-temporal pattern associated with this peak is well simulated by a whole hierarchy of ocean models for the North Atlantic's wind-driven circulation, with increasingly realistic physics, resolution and geometry [*Dijkstra and Ghil*, 2004; *Simonnet et al.*, 2004]. Atmospheric circulation patterns over the North Atlantic have well-known downwind effects, including over the Mediterranean and North Africa [*Mann*, 2002; *Felis et al.*, 2004; *Matthews*, 2004]. The effects over the source region of the Nile River, however, are new. It is tempting, moreover, to identify the 7-yr peak in the Nile River records with the cycle mentioned in Joseph's biblical story. The story, though, may refer just to a near-regularity of several years, rather than to an exact periodicity.

In Fig. 2 we plot the reconstruction of the 7-yr mode in the two extended records in which it is highly significant. The mode's amplitude varies dramatically during the time interval of interest. Several features of this amplitude modulation are common to both records, especially the increase in amplitude at about A.D. 950 and the decrease at 1450. The latter might be affected by the immediately following data gap; still, a close examination of Figs. 2a and 2b shows that large-amplitude episodes of the 7-yr mode do not necessarily coincide with intervals of abundant data in the 18th and 19th centuries. Our findings are in general agreement with those of *Fraedrich and Bantzer* [1991], who used 100-yr-long sliding windows to show that fluctuations in the 7–10-yr band tend to have large amplitudes from about A.D. 800 to roughly A.D. 1450 [see their Fig. 3].

Figure 3 shows the evolution in time of the instantaneous frequencies of the oscillatory pairs that lie in the low-frequency (40–100 yr) range. Transitions in the instantaneous frequencies of the oscillatory components are tracked by the multi-scale version of SSA [*Yiou et al.*, 2000], which has been shown to improve upon standard wavelet methods for such tracking [*Ghil et al.*, 2002].

Drastic changes occur in the dominant lower frequency around A.D. 1000 (all records), 1250 (high-water and difference), and 1500 (also the latter). Several authors [*De Putter et al.*, 1998; *Fraedrich et al.*, 1997], who used different analysis methods, all found evidence of climate shifts at the beginning and/or at the end of the Medieval Warm Period. Our results in Figs. 2 and 3 suggest that these shifts were fairly abrupt and affected several climatic modes.

4. Conclusions

The periodicities shared by the present analysis of Nile River records and global or North Atlantic modes of ocean or coupled ocean–atmosphere variability [*Ghil and Vautard*, 1991; *Schlesinger and Ramankutty*, 1994; *Dijkstra and Ghil*, 2004; *Simonnet et al.,* 2004] do not demonstrate a causal relationship. Our results suggest, though, quite strongly that the climate of East Africa has been subject to influences from the North Atlantic, besides those already documented from the Tropical Pacific [*Walker*, 1910; *Quinn*, 1992; *Kumar et al.* 1999] and those of possibly astronomical origin (*Hameed*, 1984; *De Putter et al.,* 1984; *Mann et al.*, 1995; *Vaquero et al.*, 1997]. Moreover, the fairly sharp shifts in the amplitude and period of the interannual and interdecadal modes over the last millennium-and-a-half support concerns about the possible effect of climate shifts in the not-so-distant future [Alley *et al., 2003*].

References

Allen, M. R., and L. A. Smith (1996), Monte Carlo SSA: Detecting irregular oscillations in the presence of coloured noise. *J. Clim., 9*, 3373–3404.

Alley, R. B., *et al.* (2003) Abrupt climate change, *Science, 299*, 2005–2010.

Broomhead, D. S., and G. P. King (1986), Extracting qualitative dynamics from experimental data. *Physica D*, *20*, 217–236.

Da Costa, E. D., and A. Colin de Verdière (2002), The 7.7-year North Atlantic oscillation, *Q. J. R. Meteorol. Soc., 128A*, 797–817.

De Putter, T., M. F. Loutre, and G. Wansard (1998), Decadal periodicities of Nile River historical discharge (A.D. 622–1470) and climatic implications, *Geophys. Res. Lett., 25*, 3193–3196.

Dijkstra, H. A., and M. Ghil (2004), Low-frequency variability of the large-scale ocean circulation: A dynamical systems approach, *Rev. Geophys.,* conditionally accepted.

Felis, T., et al. (2004), Increased seasonality in Middle East temperatures during the last interglacial period. *Nature, 429*, 164–168.

Fraedrich, K., and Ch. Bantzer (1991), A note on fluctuations of the Nile River flood levels *Theor. Appl. Climatol., 44*, 167–171.

Fraedrich, K., J. Jiang, F. W. Gerstengarbe, and P. C. Werner (1997), Multiscale detection if abrupt climate changes: Application to River Nile flood levels, *Int. J. Climatol., 17*, 1301–1315.

Hameed, S. (1984), Fourier analysis of Nile flood levels, *Geophys. Res. Lett., 1*, 843–845.

Hassan, F. A. (1981), Historical Nile floods and their implications for climatic change, *Science, 212*, 1142–1145.

Hurst, H. E. (1952), *The Nile*, 326 pp., Constable, London.

Ghaleb, K. O. (1951), *Le Mikyas ou Nilomètre de l'île de Rodah*. Mémoires de l'Institut d'Egypte, *54*, 182 pp. Cairo.

Ghil, M., and R. Vautard (1991), Interdecadal oscillations and the warming trend in global temperature time series, *Nature, 350*, 324-327.

Ghil, M., *et al.* (2002), Advanced spectral methods for climatic time series, *Rev. Geophys. 40(1),* 3.1–3.41, doi: 10.1029/2000GR000092 (2002).

Kumar, K. K., B. Rajagopalan, and M. A. Cane (1999), On the weakening relationship between the Indian monsoon and ENSO, *Science, 284*, 2156–2159.

Matthews, A. J. (2004), Intraseasonal variability over Tropical Africa during northern summer. *J. Climate, 17*, 2427–2440.

Mann, M. (2002), Large-scale climate variability and connections with the Middle East in past centuries, *Climatic Change, 55*, 287-314.

Mann, M., J. Park, and R. S. Bradley (1995), Global interdecadal and century-scale climate oscillations during the past five centuries, *Nature, 378*, 266–270.

Mann, M., and J. M. Lees (1996), Robust estimation of background noise and signal detection in climatic time series. *Clim. Change, 33*, 409–445.

Moron, V., R. Vautard, and M. Ghil (1998), Trends, interdecadal and interannual oscillations in global sea-surface temperatures, *Clim. Dyn., 14*, 545–569.

Popper, W. (1951), *The Cairo Nilometer*, 269 pp., University of California Press, Berkeley/Los Angeles.

Quinn, W. H. (1992), A study of Southern Oscillation-related climatic activity for A.D. 622–1900 incorporating Nile River flood data, in *El Niño*: *Historical and Paleoclimatic Aspects of the Southern Oscillation*, edited by H.F. Diaz and V. Markgraf, pp. 119–149, Cambridge Univ. Press, Cambridge.

Said, R. (1993), *The River Nile, Geology, Hydrology and Utilization*, 320 pp., Pergamon Press.

Schlesinger, M. E., and N. Ramankutty (1994), An oscillation in the global climate system of period 65–70 years, *Nature, 367*, 723–726.

Schoellhamer, D. (2001), Singular spectrum analysis for time series with missing data, *Geophys. Res. Lett.*, *16*, 3187–3190.

Simonnet, E., Ghil, M. and Dijkstra, H. A. (2004), Homoclinic bifurcations in the quasi-geostrophic double-gyre circulation, *J. Mar. Res.*, submitted.

Thomson, J. D. (1982), Spectrum estimation and harmonic analysis. *Proc. IEEE, 70*, 1055–1096.

Toussoun, O. (1925), *Mémoire sur l'histoire du Nil*, Mémoires de l'Institut d'Egypte, *18*, pp. 366–404, Cairo.

Vaquero, J. M., M. C. Gallego, and J. A. Garcia (1997), A 250-year cycle in naked-eye observations of sunspots, *Geophys. Res. Lett., 29.*, doi:10.1029/2002GL014782, 2002

Vautard, R., P. Yiou, and M. Ghil (1992), Singular-spectrum analysis: A toolkit for short, noisy chaotic signals, *Physica D, 58*, 95–126.

Walker, G. T. (1910), Correlation in seasonal variations of weather, II, *Indian Meteorol. Mem., 21*, 1–21.

Wunsch, C. (1999), The interpretation of short climate records, with comments on the North Atlantic and Southern Oscillations, *BAMS,* 245–255.

Yiou, P., D. Sornette, and M. Ghil (2000), Data-adaptive wavelets and multi-scale SSA, *Physica D, 142*, 254–290.
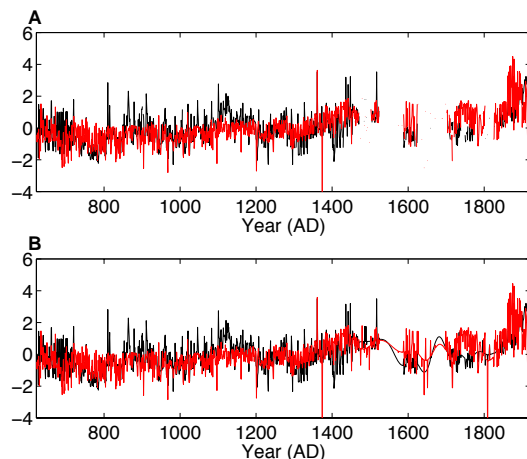

Figure 1. Extended records (AD 622–1922) of low-water (solid black curve) and high-water (solid red) levels; (a) original data; and (b) data with missing points imputed by M-SSA. The time series have been centered on the relevant mean and the amplitudes have been normalized by the standard deviation of the original time series (excluding missing data points); the variance of the high-water record is 6586 cm^2, while it is 10359 cm^2 for the low-water record.
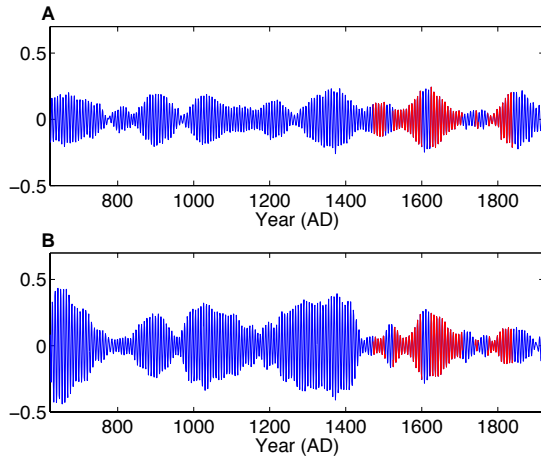
Figure 2. SSA reconstruction of the 7.2-yr mode in the extended Nile River records: (a) high-water, and (b) difference. The amplitude has been normalized by one standard deviation of the detrended time series; the variances equal 2908 cm^2 for the high-water record and 5723 cm^2 for the difference. Reconstruction in the large gaps is indicated in red.
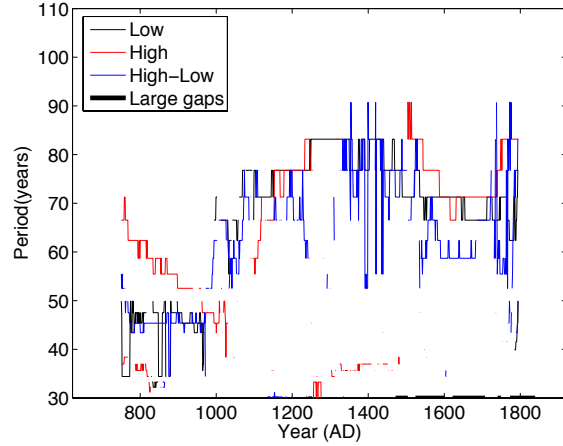

Figure 3. Temporal evolution of the instantaneous frequencies of the oscillatory pairs that lie in the low-frequency range (40–100 yr), for the low-water, high-water, and difference records. The plots are based on multi-scale SSA [Yiou et al., 2000] results with a sliding window of W = 255 yr and M = 85 yr; local SSA analysis is performed in each window of width W, with M lags. Heavy solid segments along the axis indicate large gaps with very few data points.

Table 1. Significant oscillatory modes in Nile river records. The main entries give the periods in years: bold entries without brackets indicate that the mode is significant at the 95% level against a null hypothesis of red noise, in both SSA and MTM results; entries in square brackets are significant at this level only in the MTM analysis. Entries in parentheses provide the percentage of variance captured by the mode with the given period.

Period	Low	High	Difference
a)*Short Records (A.D. 622–1470)*			
40–100 yr	**64** (9.3%)	**64** (6.9%)	**64** (6.6%)
20–40 yr		[32]	
10–20 yr	**12.2** (5.1%)		**12.2** (4.7%)
	18 (6.7%)		**18.3** (5.0%)
5–10 yr	**6.2** (4.3%)	**7.2** (4.4%)	**7.3** (4.4%)
0–5yr	**3.0** (2.9%)	**3.6** (3.6%)	**2.9** (4.2%)
	2.2 (2.3%)	**2.9** (3.4%),	
		2.3 (3.1%)	
b)*Extended records (A.D. 622–1922)*			
40–100 yr	**64** (13%)	**85** (8.6%)	**64** (8.2%)
20–40 yr		**23.2** (4.3%)	
10–20 yr	**19.7** (5.9%)		**18.3** (4.2%)
	[12]		**12.2** (4.3%)
5–10 yr	[6.2]	**7.3** (4.0%)	**7.3** (4.1%)
0–5yr	**3.0** (4%)	**4.2** (3.3%)	[4.2], **2.9** (3.6%)
	2.2 (3.3%)	**2.9** (3.3%)	**2.2** (2.6%)
		2.2 (2.9%)	